JOURNAL OF CATALYSIS 150, 400–406 (1994)

Effects of Dispersion and Metal–Metal Oxide Interactions on Fischer–Tropsch Synthesis over Ru/TiO_2 and TiO_2-Promoted Ru/SiO_2

Takashi Komaya,*,[1] Alexis T. Bell,* Zara Weng-Sieh,† Ronald Gronsky,† Frank Engelke,‡ Terry S. King,‡ and Marek Pruski‡

*Chemical Sciences Division, Lawrence Berkeley Laboratory, and Department of Chemical Engineering, University of California, Berkeley, California 94720; †Materials Science Division, Lawrence Berkeley Laboratory, and Department of Materials Science and Mineral Engineering, University of California, Berkeley, California 94720; and ‡Institute of Physical Research and Technology, Ames Laboratory, and Department of Chemical Engineering, Iowa State University, Ames, Iowa 50011

Received April 12, 1994; revised August 16, 1994

The activity of Ru/TiO_2 and TiO_2-promoted Ru/SiO_2 catalysts for Fischer–Tropsch synthesis has been investigated. The Ru dispersion of these catalysts was determined by TEM, and the fraction of the Ru surface available for H_2 adsorption was determined by ^1H NMR. Even after low-temperature reduction, the surface of titania-containing catalysts is covered by titania to a substantial degree. The specific activity and selectivity of these catalysts are dominated by the interactions occurring between the Ru particles and the titania overlayer. As the fraction of the Ru particle surface covered by titania increases, the turnover frequency for CO consumption passes through a maximum, while that for methane formation decreases monotonically. The probability for chain growth and the olefin-to-paraffin ratio of the products increase with increasing titania coverage. These trends are attributed to the effects of the titania overlayer on the catalytic properties of Ru.

INTRODUCTION

The specific activity of transition metals for Fischer–Tropsch synthesis has been found to depend on the dispersion of the metal and the composition of the support [see, for example, Ref. (1)]. The turnover frequencies for CO consumption, N_{CO}, and methane formation, N_{C_1}, decrease with increasing metal dispersion. This trend has been ascribed to the more rapid dissociation of adsorbed CO on sites associated with low index planes, which are prevalent on large particles, rather than on corner and edge sites, which are prevalent on small particles. Variations in N_{CO} and N_{C_1} with support composition are also well established, with SiO_2 and Al_2O_3 usually reported as the least active supports and titania as the most active (2–6). Investigations of the manner in which titania enhances the activity of the dispersed metal suggest that exceptionally active sites occur at the boundary between the metal and the support (2–8). At metal sites adjacent to the metal oxide, carbon monoxide can adsorb in such a fashion that the carbon end of the molecule is bonded to the metal, while the oxygen end interacts with Ti^{4+} or Ti^{3+} cations exposed at the edge of the oxide. The latter interaction can be thought of as a Lewis acid–base interaction and contributes to the dissociation of the C–O bond, the first step in the hydrogenation of CO to methane and higher molecular weight hydrocarbons. This interpretation of the enhancement in the Fischer–Tropsch synthesis activity of a metal is supported by recent studies with planar model catalysts consisting of a metal foil decorated with submonolayer quantities of titania (9–20). An alternative interpretation is that intermediates formed on the metal spillover onto the oxide, where they undergo hydrogenation to methane more rapidly than on the metal surface (21, 22).

The extent to which the Fischer–Tropsch synthesis activity of titania-supported transition metals is influenced by metal dispersion as opposed to metal–titania interaction is difficult to ascertain. During catalyst preparation and reduction the metal particles are decorated with titania moieties derived from the support and can undergo partial encapsulation by amorphous titania. The extent of metal particle encapsulation has recently been measured for Ru/TiO_2 (23). The dispersion of Ru was determined from high-resolution TEM micrographs, whereas the fraction of the Ru surface available for H_2 chemisorption was determined by ^1H NMR. As the temperature of catalyst reduction was increased from 473 to 773 K, the size of the Ru particles remained constant but the fraction of the Ru particle surface available for H_2 adsorption decreased from 50 to 15%. TEM observations revealed that

[1] Permanent address: Production Technology and Engineering Center, Mitsubishi Kasei Corporation, Kurosaki, Yahata-nishi-ku, Kitakyushu, Fukuoka 806, Japan.

0021-9517/94 $6.00

with increasing reduction temperature the Ru particles are encapsulated by an amorphous titania layer to an increasing degree, with smaller particles undergoing encapsulation more readily than larger ones.

The aim of the present instigation was to identify the effects of titania coverage of Ru particles on the activity and selectivity of Ru for Fischer–Tropsch synthesis and to determine how important these effects might be relative to the dispersion of Ru. Both Ru/TiO_2 and TiO_2-promoted Ru/SiO_2 catalysts were used. The Ru dispersion of each catalyst was determined by transmission electron microscopy (TEM) and the fraction of the Ru surface available for H_2 chemisorption was determined by ^1H NMR.

EXPERIMENTAL

Catalyst Preparation

Titania-supported Ru catalysts were prepared by incipient wetness impregnation of TiO_2 (Degussa P-25) with an aqueous solution of $Ru(NO)(NO_3)_3$ (Johnson–Matthey). The impregnated TiO_2 was air dried at 383 K for 16 h and then sieved to 30–60 mesh. The dried catalyst was reduced at 523 K in a flow of H_2 and passivated in He containing 1000 ppm of O_2 at room temperature. The reduced catalyst was washed repeatedly in boiling water to remove Na, a contaminant in the Ru precusor. The washed catalyst was dried at 383 K in vacuum for 3 h and rereduced at 523 K in a flow of H_2, after which it was again passivated. The final catalysts prepared in this manner are referred to as Ru/TiO_2 (M-1) and Ru/TiO_2 (H-1). Another sample of titania-supported Ru, designated Ru/TiO_2 (L-1), was prepared by impregnation of TiO_2 with an excess of an aqueous solution of $Ru(NO)(NO_3)_3$ at pH 8, followed by filtration and water rinsing of the impregnated TiO_2. This sample was then dried, reduced, washed with boiling water, and reduced again in the same manner as the two other Ru/TiO_2 catalysts. The weight loading of Ru was determined by X-ray fluorescence. The weight loadings are 1.5% for Ru/TiO_2 (L-1), 4.8% for Ru/TiO_2 (M-1), and 6.7% for Ru/TiO_2 (H-1).

A TiO_2-promoted Ru/SiO_2 sample was prepared in the following manner. A 4.9% Ru/SiO_2 catalyst, designated (TS-1), was prepared by following the same procedure used to prepare Ru/TiO_2 (H-1). Cab-O-Sil L-90 was used as the support in this case. The silica-supported catalyst was then impregnated with an isopropanol solution of $Ti(OC_3H_7)_4$ (DuPont), prepared in a dry N_2 atmosphere, by dropwise addition to the point of incipient wetness. The impregnated sample was oxidized in air at 383 K for 3 h and reduced at 523 K in a flow of H_2, after which it was passivated. The final catalysts are reffered to as $TiO_2/Ru/SiO_2$ (TS-2) and $TiO_2/Ru/SiO_2$ (TS-3). The amount of $Ti(OC_3H_7)_4$ added corresponded to a Ti weight loading of 1.9 and 7.2%, respectively.

Catalyst Characterization

The dispersion of the supported Ru particles was determined by TEM. The catalysts were ground to a fine powder and then dry-dispersed onto a carbon-coated copper grid. Micrographs were obtained on a Topcon 002B transmission electron microscope operated at 200 KV, with a nominal point-to-point resolution of 1.9 Å. Ru particles were identified by using a combination of selected-area diffraction techniques and measurement of the lattice-fringe spacings. The average Ru particle size was determined from image-processing analysis of about 100 particles and the dispersion was determined from the average particle size.

Characterization of the fraction of the Ru surface sites available for H_2 chemisorption was determined from ^1H NMR measurements obtained with a home-built spectrometer operating at a resonance frequency of 250 MHz. Sealed samples were placed in a ^1H NMR probe constructed at Ames Laboratory following the design of Haddix *et al.* (24). Additional details concerning the NMR experiments are given in Ref. (23).

About 100 mg of catalyst, which had been used for Fischer–Tropsch synthesis and then passivated in He containing 1000 ppm of O_2, was placed in a 5-mm-o.d. NMR tube attached to one of the sample ports of an adsorption apparatus. The sample was then reduced at 523 K for 2 h in 760 Torr of H_2. After reduction, the sample was evacuated for 1 h at the reduction temperature and cooled to room temperature. The sample was then dosed with H_2 at 400 Torr, equilibrated for 30 min, and evacuated to 10^{-5} Torr for 10 min. Finally, the sample was immersed in a water bath and sealed with a microtorch. The sample preparation conditions were chosen to have minimal effect on the titania overlayer covering the Ru particles (see below).

The spectrum of H_2 adsorbed on Ru is characterized by a peak at -56 to -78 ppm. The position of this line is dominated by the Knight shift, which decreases as the Ru particles become larger. For quantification of the amount of H_2 adsorbed on Ru, the observed signal is compared with that of water slightly doped with $FeCl_3$ (23). The fraction of the surface available for H_2 chemisorption is calculated as the ratio of H_i/Ru_t to Ru_s/Ru_t, where H_i is the moles of irreversibly adsorbed H_2 per gram of catalyst and Ru_s and Ru_t are the moles of surface and total Ru, respectively, per gram of catalyst. The fraction of the catalyst covered by TiO_x is given by $\theta_{TiO_x} = 1 - (H_i/Ru_s)$.

Reaction Apparatus

All reactions were carried out in a low dead volume quartz microreactor supplied with H_2 and CO from a gas

manifold. UHP H_2 (Matheson Gas) was further purified by passage through a Deoxo unit (Engelhard Industries) and water was removed by a molecular sieve 13× trap. UHP CO (99.999% pure, Matheson Gas) was passed through a glass bead trap maintained at 573 K to remove iron carbonyls, an Ascarite trap to remove CO_2, and a molecular sieve trap to remove water. The reaction products were analyzed by gas chromatography using a fused silica capillary column (0.25 mm i.d. × 50 m) coated with a 1-μm film of SE-54. In all experiments, the CO conversion was less than 5%, and more usually less than 1%. Steady-state distribution of C_3-C_9 products were achieved within the first 10 min under reaction conditions.

RESULTS

Table 1 lists characteristics of the three Ru/TiO_2 catalysts determined after exposure of each catalyst to reaction conditions. While the dispersions of the 4.8% Ru/TiO_2 and 6.7% Ru/TiO_2 catalysts are stable under reaction conditions, the dispersion of the 1.5% Ru/TiO_2 decreased from 100 to 77% during 200 min of reaction, but remained constant thereafter. For 1.5% Ru/TiO_2, only 15% of the Ru particle surface is available for H_2 chemisorption after the first 40 min under reaction conditions. This fraction rises, though, to 49% as the particles sinter. By contrast, for the 4.8% Ru/TiO_2 and 6.7% Ru/TiO_2 samples the fraction of the Ru particle surface available for H_2 chemisorption is invariant with the length of time under reaction conditions, remaining at 51 and 56%, respectively.

The characteristics of the TiO_2-promoted Ru/SiO_2 catalysts are listed in Table 2. The dispersion of Ru is unaffected by either TiO_2 promotion or exposure of the catalysts to reaction conditions. As the level of TiO_2 promotion increases, the fraction of the Ru particle surface available for H_2 chemisorption decreases from 100 to 54%.

Figure 1 shows a plot of N_{CO} and N_{C_1} versus Ru dispersion for the Ru/TiO_2 catalysts. For this plot the turnover frequencies are based on the total number of sites present at the surface of the Ru particles, neglecting the effects of particle encapsulation by titania. This basis for determining the turnover frequencies was chosen to facilitate comparison of the present results with those reported in the literature (see below). As seen in Fig. 1, the values of

TABLE 1

Characteristics of Ru/TiO_2 Catalysts

Ru/TiO_2 catalyst	L-1[a]	L-3[b]	L-5[c]	M-1[d]	H-1[d]
Ru loading (wt%)	1.5	1.5	1.5	4.8	6.7
Ru particle size (Å)	8	22	13	15	20
Ru dispersion[a]	1.00	0.91	0.77	0.67	0.50
H_i/Ru_t[e]	0.15	0.27	0.38	0.34	0.28
θ_{TiO_x}[f]	0.85	0.70	0.51	0.49	0.44

[a] First exposure to reaction conditions (T = 483 K; P = 1 atm; D_2/CO = 3; 40 min).

[b] Third exposure to reaction conditions.

[c] Fifth exposure to reaction conditions. (The catalyst activity and selectivity were stable for all subsequent exposures to reaction conditions.)

[d] First exposure to reaction conditions. (The catalyst activity and selectivity were stable for all subsequent exposures to reaction conditions.)

[e] Irreversible uptake of H_2 determined by ^1H NMR (see text).

[f] Coverage of the Ru particle surface by TiO_x (see text).

TABLE 2

Characteristics of $TiO_2/Ru/SiO_2$ Catalysts

Ru/TiO_2 catalyst	TS-1[a]	TS-2[a]	TS-3[a]	M-1[a]
Ru loading (wt%)	4.9	4.8	4.5	4.8
TiO_2 loading (wt%)	0.0	1.9	7.2	95.2
Ru particle size (Å)	35	35	35	15
Ru dispersion	0.28	0.28	0.28	0.67
H_i/Ru_t[b]	0.25	0.22	0.15	0.34
θ_{TiO_x}[f]	0.0	0.21	0.46	0.49

[a] The catalyst was characterized after a single exposure to reaction conditions (T = 483 K; P = 1 atm; D_2/CO = 3; 40 min). Subsequent exposure of the catalyst to reaction conditions did not alter the catalyst activity or selectivity.

[b] Irreversible uptake of H_2 determined by ^1H NMR (see text).

[c] Coverage of the Ru particle surface by TiO_x (see text).

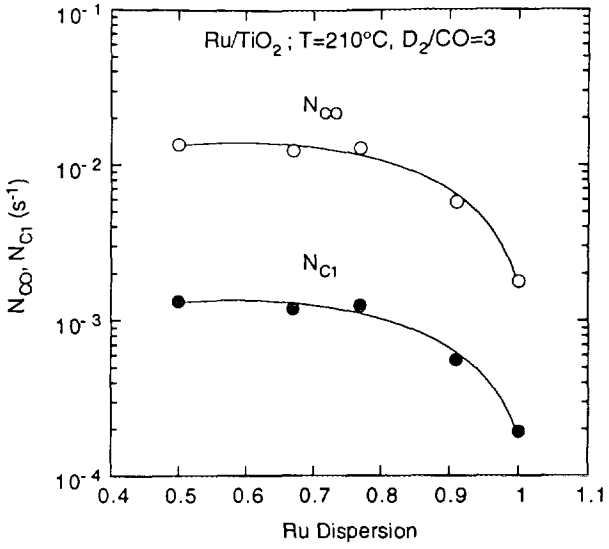

FIG. 1. Turnover frequencies for CO consumption, N_{CO}, and CH_4 formation, N_{C_1}, as a function of Ru dispersion. The turnover frequencies are based on the Ru dispersion.

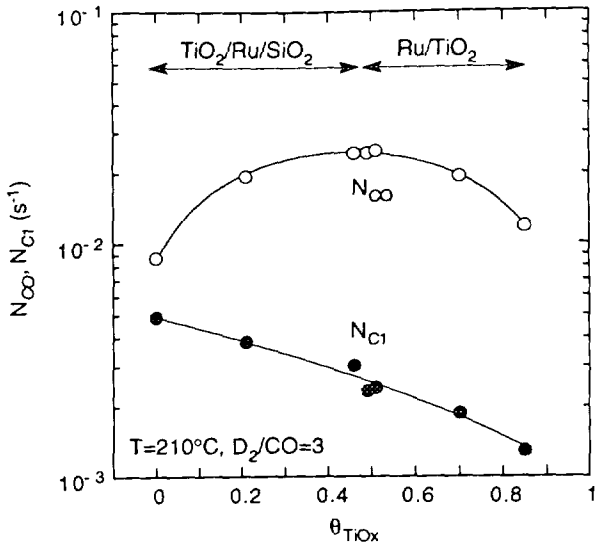

FIG. 2. Turnover frequencies for CO consumption, N_{CO}, and CH_4 formation, N_{C_1}, as a function of TiO_x coverage. The turnover frequencies are based on Ru surface sites available for H_2 chemisorption.

N_{CO} and N_{C_1} are nearly independent of dispersion for $D_{Ru} < 0.75$ but then decrease for $D_{Ru} > 0.75$.

The turnover frequencies for CO consumption and the formation of methane (C_1) are shown in Fig. 2 as a function of the coverage of the Ru particle surface by TiO_x, θ_{TiO_x}, for both the Ru/TiO_2 and the TiO_2-promoted Ru/SiO_2 catalysts. In this case both N_{CO} and N_{C_1} are defined in terms of the fraction of the Ru surface sites available for chemisorption. What is remarkable is that the data for TiO_2-promoted Ru/SiO_2 and Ru/TiO_2 converge at $\theta_{TiO_x} = 0.5$. The value of N_{CO} rises from 9×10^{-3} s^{-1} up to 2.5×10^{-2} s^{-1} as the value of θ_{TiO_x} increases from 0 to 0.5, and then decreases as θ_{TiO_x} approaches unity. By contrast, the value of N_{C_1} decreases monotonically from 5×10^{-3} s^{-1} as θ_{TiO_x} increases from 0. Catalyst samples for which θ_{TiO_x} is approximately 0.5 exhibit the same values of N_{CO} and N_{C_1}, independent of the Ru dispersion. For example, reference to Tables 1 and 2 shows that sample L-5 has a dispersion of 77% ($\theta_{TiO_x} = 0.51$), whereas sample TS-3 has a dispersion of 28% ($\theta_{TiO_x} = 0.46$).

The effects of θ_{TiO_x} on the probability of chain growth, α, and on the olefin to paraffin ratio are presented in Figs. 3 and 4, respectively. The value of α presented in Fig. 3 increases monotonically from 0.41 to 0.75 as θ_{TiO_x} increases from 0 to 0.85. Figure 4 shows that the olefin to paraffin ratio for C_2 and C_4 products increase by over an order of magnitude as θ_{TiO_x} increases from 0 to 0.85. Here again, the data for TiO_2-promoted Ru/SiO_2 and Ru/TiO_2 are consistent, and no evidence is found for the dependence of the value of α or the olefins to paraffin ratio on the Ru dispersion.

To obtain a more detailed understanding of the effects of TiO_x coverage on the dynamics of hydrocarbon chain initiation, growth, and termination, isotopic tracer experiments were carried out under steady-state conditions. These experiments give curves of $F_n(t)$, the fraction of the product labeled with ^{13}C as a function of time, for values of $n = 2$–8. Simulation of these curves based on a model of the dynamics of chain initiation, growth, and termination (25) allows us to determine the values of the rate coefficients for chain initiation, k_i, propagation, k_p,

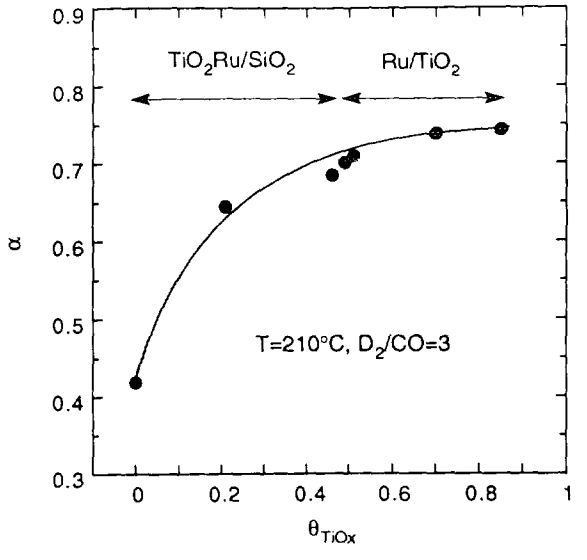

FIG. 3. The probability of chain growth, α, as a function of TiO_x coverage.

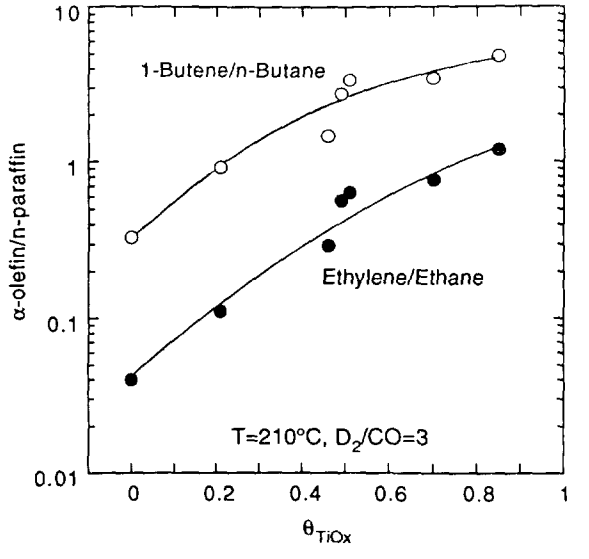

FIG. 4. The olefin to paraffin ratio for C_2 and C_4 products as a function of TiO_x coverage.

and termination, k_t, and to determine the coverage of the Ru surface by monomeric species (CH_2), chain initiators (CH_3), and growing chains (C_nH_{2n+1}). The results of these simulations are presented in Figs. 5 and 6.

The values of k_i, k_p, and k_t are shown in Fig. 5 as a function of θ_{TiO_x}. The value of k_i decreases monotonically with increasing TiO_x coverage. While the value of k_p is essentially independent of θ_{TiO_x}, the value of k_t decreases to a plateau as the value of θ_{TiO_x} increases from 0 to 0.5. The values of k_p and k_t given in Fig. 5 are an average of the values observed for $n = 2$–8, which were essentially independent of carbon number (25). Figure 6 shows the values of θ_m, θ_1, and θ_n for n between 2 and 12. Each of these quantities exhibits a unique dependence on θ_{TiO_x}.

DISCUSSION

Studies of CO hydrogenation over Ru/Al_2O_3 have shown that the turnover frequencies for CO consumption and methane formation decrease as the dispersion of Ru increases (1, 26, 27). Similar trends have also been reported recently for Ru/TiO_2 (28). The latter results need to be viewed with some care, though, since both the dispersion and the number of sites for determination of the turnover frequencies were based on measurements of irreversibly chemisorbed H_2. As recently demonstrated by Komaya *et al.* (23), volumetric determinations of H_2 on Ru/TiO_2 give erroneous measures of Ru dispersion due to the spillover of H_2 onto the support and the partial occlusion of Ru by amorphous titania. The first of these effects leads to an overestimation of the true dispersion of the metal, whereas the second effect leads to an underestimation of the true metal dispersion. Nevertheless, even if one allows for some correction due to these effects, the direction of the trend between turnover frequency and Ru dispersion is unaltered. The results of the present study given in Fig. 1 show that if the total number of Ru sites on the surface of the Ru particles is used to calculate the turnover frequencies for CO consumption and methane formation, then one again observes an inverse effect of Ru dispersion on N_{CO} for $D_{Ru} > 0.75$, but no effect of dispersion for $D_{Ru} < 0.75$.

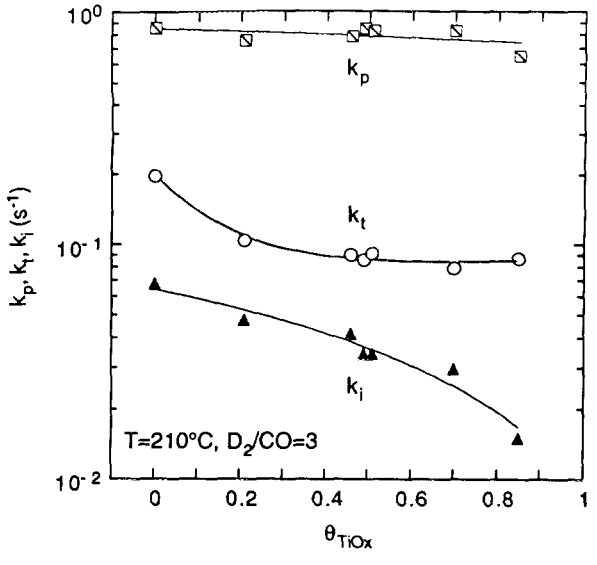

FIG. 5. The rate coefficients for chain initiation, k_i, chain propagation, k_p, and chain termination, k_t, as a function of TiO_x coverage.

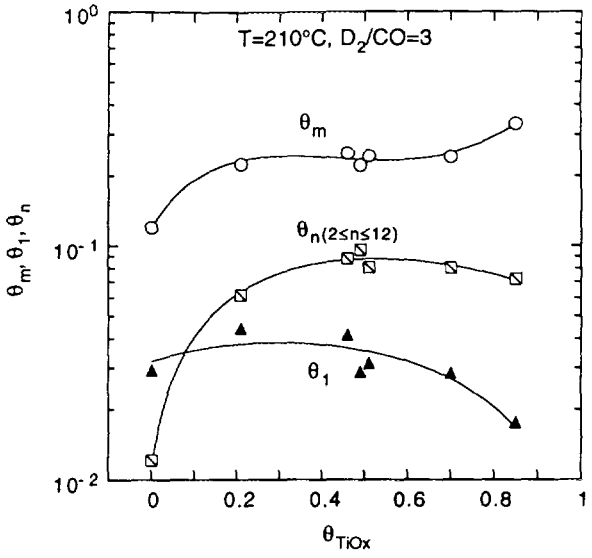

FIG. 6. The surface coverages by C_1, C_n ($n = 2$–12), and CH_2 species as a function of TiO_x coverage.

The central question to be addressed is whether Ru dispersion or the interaction of Ru with titania is the dominant factor controlling the catalytic properties of titania-supported or titania-promoted Ru. This issue can be addressed by examining the performance of catalysts having the same dispersion but different coverages of titania and by examining the performance of different catalysts having the same titania coverage but different Ru dispersions. The data in Figs. 1–3 and Table 2 clearly demonstrate that promotion of Ru/SiO_2 with titania has no effect on the Ru dispersion but enhances the values of N_{CO}, N_{C_1}, α, and the olefin-to-paraffin ratio. Likewise, consideration of the data in Tables 1 and 2 and Figs. 1–3 leads to the observation that for θ_{TiO_x} close to 0.5 the values of N_{CO}, N_{C_1}, α, and the olefin-to-paraffin ratio are virtually the same for Ru/TiO_2 and TiO_2-promoted Ru/SiO_2 catalysts exhibiting Ru dispersions between 0.28 and 0.77. Taken together, these observations suggest that the interactions of titania with Ru control the catalytic properties of Ru to a much larger degree than the effects of dispersion. A possible reason for this is that the

smaller, intrinsically less active, particles of Ru are completely encapsulated by titania and hence are totally inactivated. This picture is strongly supported by the recent findings of Komaya *et al.* (23) which shows that small particles of Ru are encapsulated to a much higher level than are larger Ru particles. A similar trend is seen in the data presented in Table 1 which shows that as the 1.5% Ru/TiO_2 catalyst undergoes sintering, a progressively larger fraction of the surface Ru atoms becomes exposed; i.e., θ_{TiO_x} decreases. What this suggests is that only the larger, more active Ru particles avoid extensive encapsulation and, consequently, participate significantly in Fischer–Tropsch synthesis.

The mechanism by which TiO_x enhances the activity of transition metals for CO hydrogenation has been discussed extensively in the literature (2–20). The accumulated evidence suggests that CO can adsorb at the titania-metal boundary in such a fashion that the carbon end of the molecule is bound to the metal while the oxygen end of the molecule interactions with exposed Ti^{3+} or Ti^{4+} cations. The latter form of interaction is believed to involve the formation of a Lewis acid–base adduct. CO molecules adsorbed at the titania–metal boundary exhibit lower CO stretching frequencies, suggesting a weakening of the C–O bond. Facilitation of the rupture of the C–O bond enhances the rate of formation of adsorbed carbon atoms, the first intermediate along the path to hydrocarbons. In a recent study of the effects of various metal oxides on the catalytic activity of a Rh foil for CO hydrogenation, it was observed that titania is one of the most effective promoters (20). The high effectiveness of titania was attributed to the high electronegativity of the Ti cations.

Studies conducted with alumina-supported transition metals (21, 22, 29–31) have suggested that methane may form via two pathways, one involving hydrogenation of intermediates on the metal surface and the other involving spillover of the intermediates onto the alumina and subsequent hydrogenation on the support. In the case of Pt/Al_2O_3 and Pd/Al_2O_3, methane is observed to form more readily via the second than the first of the two process, whereas on Ni/Al_2O_3 the reverse is true. No evidence for a spillover mechanism has been reported for titania-supported metals. The liklihood that a spillover mechanism could explain the results reported in this study seems doubtful. Ru has an intrinsic activity more comparable to Ni than Pt, and hence, even if spillover onto the titania occurred, the rate of hydrogenation of these species to methane would be expected to be slower than that occurring on the metal surface.

Figure 2 exhibits a maximum in N_{CO} versus θ_{TiO_x}. This pattern is identical to that seen in the turnover frequency for methane formation from CO and H_2 over a titania-promoted Rh foil (20). In this case the selectivity to methane is nearly 100% and the turnover frequency is calculated on the basis of the surface area of the unpromoted foil. However, even if one recalculates the turnover frequency for methane formation on the basis of the Rh surface area free of titania, the turnover frequency still passes through a maximum at about $\theta_{TiO_x} = 0.5$. The presence of a maximum for both titania-promoted Rh foil and supported Ru particles is attributable to the need for both exposed metal sites and cationic sites at the metal–oxide boundary for both exposed metal sites and cationic sites at the metal–oxide boundary for CO hydrogenation. Exposed metal sites are required for the adsorption of H_2, whereas a combination of metal and cation sites situated along the metal–oxide boundary are required for high rates of C–O bond dissociation.

As θ_{TiO_x} increases, the number of exposed Ru sites at the surface of the Ru particles decreases. Since these sites are the ones on which H_2 adsorbs, they are essential for the supply of adsorbed hydrogen required for hydrogenation of alkyl species. The monotonic fall off in the rate of methane formation with increasing θ_{TiO_x}, as well as the rise in the olefin-to-paraffin ratio of the products, can be ascribed to the decrease in the availability of adsorbed H_2. A decrease in the number of exposed Ru sites would also reduce the rate of chain termination via either β-hydrogen elimination from alkyl groups to form olefins or α-hydrogen addition to alkyl groups to form paraffins. Consistent with this one observes a monotonic increase in the value of α (see Fig. 2) as θ_{TiO_x} increases.

The trends in the values of k_i, k_p, and k_t with increasing θ_{TiO_x}, seen in Fig. 4, are consistent with the above discussion. The value of k_i decreases monotonically with increasing θ_{TiO_x}. Since k_i is really a product of the intrinsic rate coefficient and the coverage of the metal surface by hydrogen, the observed decrease in k_i is attributable to the decrease in hydrogen coverage (25). The value of k_p is virtually independent of θ_{TiO_x} as one might expect, since k_p does not depend on hydrogen coverage. As discussed by Komaya and Bell (25), k_t is an effective rate coefficient for chain termination which is comprised of two terms. The first is the rate coefficient for termination to olefins and the second is the rate coefficient for termination to paraffins. The first term is proportional to the fraction of surface vacancies, whereas the second is proportional to the coverage by adsorbed hydrogen. As discussed above, the surface fractions of vacancies and adsorbed hydrogen both decrease as θ_{TiO_x} increases. The net effect of these changes is that k_t decreases with increasing θ_{TiO_x}, but at a progressively slower rate, the higher the value of θ_{TiO_x}.

CONCLUSIONS

The specific activity and selectivity of titania-supported and titania-promoted Ru catalysts are dominated

by the interactions occurring between Ru and titania, and to much lesser degree by the dispersion of Ru. As the fraction of the Ru particle surface covered by titania increases the turnover frequency for CO consumption passes through a maximum, while that for methane formation decreases monotonically. The probability for chain growth, α, and the olefin to paraffin ratio of the products increase significantly with increasing θ_{TiO_x}. The observed trends are attributable to the balance between Ru surface sites present along the boundary between Ru and titania, and the Ru surface sites unaffected by titania. The former type of site is effective in dissociating the C–O bond, a critical first step along the path to Fischer–Tropsch synthesis, whereas the latter type of site controls the availability of adsorbed hydrogen and, hence, the rate of chain termination and the olefin-to-paraffin ratio.

ACKNOWLEDGMENTS

This work was supported by the Office of Chemical Sciences, Division of Basic Energy Sciences, of the U.S. Department of Energy under Contract DE-AC03-76SF00098 at the Lawrence Berkeley Laboratory and under Contract W-7405-Eng-82 at the Ames Laboratory. Access to the facilities at the National Center for Electron Microscopy is acknowledged. Z. Weng-Sieh gratefully recognizes support from a Noyce Foundation fellowship.

REFERENCES

1. Che, M., and Bennett, C. O., *Adv. Catal.* **36,** 55 (1989).
2. Tauster, S. J., *Acc. Chem. Res.* **20,** 389 (1987).
3. Bell, A. T., *in* "Catalyst Design–Progress and Perspectives" (L. L. Hegedus, Ed.). Wiley, New York, 1987.
4. Burch, R., *in* "Hydrogen Effects in Catalysts" (Z. Paal and P. G. Menon, Eds.), Dekker, New York, 1988.
5. Haller, G. L., and Resasco, D. E., *Adv. Catal.* **36,** 173 (1989).
6. Vannice, M. A., *Catal. Today* **12,** 255 (1992).
7. Burch, R., and Flambard, A. R., *J. Catal.* **86,** 384 (1982).
8. Sachtler, W. M. H., Shriver, D. F., Hollenberg, W. B., and Lang, A. F., *J. Catal.* **92,** 429 (1985).
9. Chung, Y.-W., Xiong, G., and Kao, C. C., *J. Catal.* **85,** 237 (1984).
10. Demmin, R. A., Ko, C. S., and Gorte, R. J., *J. Phys. Chem.* **89,** 1151 (1985).
11. Demmin, R. A., and Gorte, R. J., *J. Catal.* **98,** 577 (1986).
12. Demmin, R. A., and Gorte, R. J., *J. Catal.* **105,** 373 (1987).
13. Levin, M. E., Salmeron, M., Bell, A. T., and Somorjai., G. A., *Surf. Sci.* **169,** 123 (1986).
14. Levin, M. E., Salmeron, M., Bell, A. T., and Somorjai., G. A., *J. Catal.* **106,** 401 (1987).
15. Levin, M. E., Salmeron, M., Bell, A. T., and Somorjai., G. A., *Surf. Sci.* **195,** 429 (1988).
16. Williams, K. J., Salmeron, M., Bell, A. T., and Somorjai, G. A., *Surf. Sci.* **204,** L745 (1988).
17. Williams, K. J., Boffa, A. B., Salmeron, M., Bell, A. T., and Somorjai., G. A., *Catal. Lett.* **5,** 385 (1990).
18. Williams, K. J., Boffa, A. B., Salmeron, M., Bell, A. T., and Somorjai., G. A., *Catal. Lett.* **9,** 41 (1991).
19. Boffa, A. B., Bell, A. T., and Somorjai, G. A., *J. Catal.* **139,** 602 (1993).
20. Boffa, A. B., Bell, A. T., and Somorjai, G. A., *J. Catal.* **149,** 149 (1994).
21. Flesner, R. L., and Falconer, J. L., *J. Catal.* **139,** 421 (1993).
22. Robbins, J. L., and Marucchi-Soos, E., *J. Phys. Chem.* **93,** 2885 (1989).
23. Komaya, T., Bell, A. T., Weng-Sieh, Z., Gronsky, R., Engelke, F., King, T. S., and Pruski, M., *J. Catal.* **149,** 142 (1994).
24. Haddix, G. W., Reimer, J. A., and Bell, A. T., *J. Catal.* **106,** 111 (1987).
25. Komaya, T., and Bell, A. T., *J. Catal.* **146,** 237 (1994).
26. King, D. L., *J. Catal.* **51,** 386 (1978).
27. Kellner, C. S., and Bell, A. T., *J. Catal.* **75,** 251 (1982).
28. Krishna, K. R., and Bell, A. T., *J. Catal.* **130,** 597 (1991).
29. Glugla, P. G., Bailey, K. M., and Falconer, J. L., *J. Phys. Chem.* **92,** 4474 (1988); *J. Catal.* **115,** 24 (1989).
30. Sen, B., Falconer, J. L., Mao, T.-F., Yu, M., and Flesner, R. L., *J. Catal.* **126,** 465 (1990).
31. Hsiao, E. C., and Falconer, J. L., *J. Catal.* **132,** 145 (1991).